General Disclaimer

One or more of the Following Statements may affect this Document

- This document has been reproduced from the best copy furnished by the organizational source. It is being released in the interest of making available as much information as possible.

- This document may contain data, which exceeds the sheet parameters. It was furnished in this condition by the organizational source and is the best copy available.

- This document may contain tone-on-tone or color graphs, charts and/or pictures, which have been reproduced in black and white.

- This document is paginated as submitted by the original source.

- Portions of this document are not fully legible due to the historical nature of some of the material. However, it is the best reproduction available from the original submission.

Produced by the NASA Center for Aerospace Information (CASI)

X-611-69-123
PREPRINT

NASA TM X- 63507

PHYSICAL PROPERTIES OF THE RADIO-EMITTING REGION IN SCO X-1

GUENTER R. RIEGLER
REUVEN RAMATY

FACILITY FORM 602

N69-22113 (ACCESSION NUMBER) 1 (THRU)
14 (PAGES) (CODE)
TMX 63507 (NASA CR OR TMX OR AD NUMBER) 30 (CATEGORY)

MARCH 1969

GSFC
GODDARD SPACE FLIGHT CENTER
GREENBELT, MARYLAND

PHYSICAL PROPERTIES

of the

RADIO-EMITTING REGION in SCO X-1

by

Guenter R. Riegler*

Department of Physics and Astronomy
University of Maryland, College Park, Maryland 20742

and

Reuven Ramaty**

NASA/Goddard Space Flight Center
Greenbelt, Maryland 20771

March 1969

* Research supported by NASA Grant NGL-21-002-033
** NAS/NASA Post-doctoral Resident Research Associate

PHYSICAL PROPERTIES OF THE RADIO-EMITTING REGION IN SCO X-1

by

Guenter R. Riegler*

Department of Physics and Astronomy,
University of Maryland, College Park, Maryland 20742

Reuven Ramaty**

NASA/Goddard Space Flight Center
Greenbelt, Maryland 20771

Abstract:

On the basis of recent observations we deduce that the radio emission from Sco X-1 is synchrotron radiation of relativistic electrons in an extended low-density region surrounding a denser core which produces the X-ray and optical continua. The linear dimensions of the radio-emitting region are larger than $\approx 10^{12}$ cm, the ambient density is less than $\approx 10^{9}$ cm^{-3} and the radiation could typically be produced by electrons of about 15 MeV in a magnetic field of a few gauss.

* Research supported by NASA Grant NGL-21-002-033

** NAS/NASA Post-doctoral Resident Research Associate

PHYSICAL CHARACTERISTICS OF THE RADIO-EMITTING REGION OF SCO X-1

Radio emission from Sco X-1 at 4.6 cm and 6 cm has recently been observed by Andrew and Purton (1968) and Ables (1969). The reported radio fluxes are shown in Figure 1 together with typical spectra in the near infrared, optical and low-energy (1 - 20 keV) X-ray regions (Neugebauer et al. 1969; Gorenstein et al. 1968). The low-energy X-ray flux is consistent with a bremsstrahlung spectrum from an isothermal, optically thin plasma at a temperature that may vary from 4×10^7 °K to 10^8 °K (Gorenstein et al. 1968). The X-ray spectrum above 20 keV was also measured by a number of observers (Peterson and Jacobson 1966; Lewin et al. 1968) and was found to be consistent with a thermal source of similar temperature. Above about 35 keV. however, several experiments (Peterson and Jacobson 1966; Buselli et al. 1968; Riegler et al. 1968; Riegler 1969) have revealed an X-ray component which may vary in time and which cannot be characterized by a thermal spectrum of the type mentioned above. This component may, therefore, indicate the existence of a non-thermal radiation from Sco X-1.

Consistent models for the emission in the infrared, the visual and the low-energy X-ray bands can be obtained by assuming that the radiation is produced by a homogeneous isothermal electron distribution which is optically thin at X-ray energies and becomes optically thick in the visual and infrared regions (Chodil et al. 1968; Neugebauer et al. 1969). An exponential spectrum in the X-ray region may also be produced by synchrotron emission from an electron distribution with a sharp high-energy cutoff

(Hayakawa et al. 1966; Manley 1966). In the terms of this model, the drop in the infrared could be caused either by plasma effects (e.g. the Razin effect) or by synchrotron reabsorption. In both the bremsstrahlung and synchrotron models, however, the emission would decrease sharply below $\nu \approx 10^{14}$ Hz. The observed radio emission at $\sim 5 \times 10^{9}$ Hz, therefore, could not be produced by the same mechanism in the same physical region as that responsible for the infrared, visual and low-energy X-ray emissions.

The upper limit on the linear dimension, R, of this region, based on the upper limit of the visual size of Sco X-1 (Sandage et al. 1966; Johnson 1966) is of the order of 10^{15} cm. This value corresponds to a distance of 500 pc to Sco X-1, which we shall use throughout the present letter. Based on the separation of binary stars, however, Westphal et al. (1968) suggest that a more likely range for the linear dimensions of the object is 10^{11} to 10^{12} cm, whereas Neugebauer et al. (1969), from the observed infrared spectrum of Sco X-1, find that $R \approx 10^{9}$ cm. Using an emission measure $\frac{4\pi}{3} R^3 n^2 \approx 9.4 \times 10^{59}$ cm^{-3} (Gorenstein et al. 1968) for the low-energy X-rays, values of R ranging from 10^{15} cm to 10^{9} cm imply densities varying from 1.5×10^{7} cm^{-3} to 1.5×10^{16}.

An absolute upper limit on the density of the ambient medium in the radio-emitting region of Sco X-1 is of the order of 3×10^{11} cm^{-3}, corresponding to a plasma frequency of 5×10^{9} Hz. If the radio emission is produced in the same region as the low-energy X-rays, the linear dimensions of the object would be $\approx 1.4 \times 10^{12}$ cm. For this radius, the

brightness temperature of the radio emission is $\approx 1.4 \times 10^{10}$ °K, which is much larger than that in the low-energy X-ray region.

In the present letter we wish to suggest that the radio emission from Sco X-1 is gyro-synchrotron or synchrotron radiation, produced by a non-thermal source of energetic electrons which differ, both in energy and spatial confinement, from those producing the infrared, visual and low-energy X-ray continua. The relatively small size of Sco X-1 implies that the radio emission from this object may be significantly affected by synchrotron reabsorption, while a large ambient density requires that plasma effects be taken into account. The theory of synchrotron emission and reabsorption of ultrarelativistic electrons was treated by several authors (e.g. Ginzburg and Syrovatskii 1969). Since the radio emission from Sco X-1, however, could result from electrons of only mildly relativistic energies, we shall use the detailed theory of gyrosynchrotron emission and absorption in a magnetoactive plasma that was developed recently by Ramaty (1969).

We consider a radio source of volume $V = 4\pi/3\ R^3$ and radiating area $A = \pi R^2$ that contains a non-thermal distribution of electrons of the form

$$u(\gamma) \propto (\gamma - 1)^{-\Gamma}, \qquad (1)$$

normalized to $N\ (=n_{rel}\ V)$ particles of Lorentz factors, γ, greater than 1.2 (100 keV). We have arbitrarily assumed that $\Gamma = 3$. The radiation intensity at the source of the emission, I, as a function of ν/ν_B and for various values of the parameter N/BA and the product BN/A, is given

in Figure 2. The gyrofrequency, ν_B, is given by $\nu_B = 2.8 \times 10^6 B$, where B is the ambient magnetic field in the emitting region. At high frequencies, in the optically thin case the spectrum approaches a power law of the form ν^{-1}, whereas at frequencies at which the source is opaque, the spectrum varies like $\nu^{5/2}$. These asymptotic forms are well known from the theory of synchrotron radiation from ultrarelativistic electrons (e.g. Ginzburg and Syrovatskii 1965), but break down at low frequencies where this theory is no longer valid. From spectra such as those shown in Figure 2, as well as from synchrotron theory, it is possible to show that in the high frequency limit the frequencies of maximum emission, ν_m/ν_B, and the unnormalized intensities at these frequencies, $\phi_m = I_m A/BN$, depend only on N/BA, and are given by

$$\nu_m/\nu_B \propto (N/BA)^{\frac{2}{\Gamma + 4}} \tag{2}$$

$$\phi_m \propto (N/BA)^{-\frac{\Gamma - 1}{\Gamma + 4}} , \tag{3}$$

where the constants of proportionality are only weakly dependent functions of the spectral index Γ.

The spectra shown in Figure 2 correspond to radiation in vacuum. The ambient plasma, however, affects both the emissivity and the absorption coefficient in that at low frequencies both quantities may be significantly suppressed. The simultaneous treatment of this suppression effect, commonly referred to as the Razin effect, and gyro-synchrotron reabsorption was recently given by Ramaty (1969). To a first approximation,

the relative importance of reabsorption and the Razin effect can be determined by comparing the frequency of maximum emission, ν_m, with the Razin frequency, $\nu_R = 20\ n_e/B$, where n_e is the ambient electron density in the emitting region. If $\nu_R \ll \nu_m$, the Razin effect is negligible and the radiation is well represented by the spectra shown in Figure 2; for $\nu_R > \nu_m$ these spectra will peak at higher frequencies and at lower maximum intensities.

Since the available radio observations of Sco X-1 are not sufficient to define a frequency spectrum, we have assumed that $\nu_R < \nu_m$ and that the lowest frequency (5×10^9 Hz) at which a finite radio flux was observed is actually equal to the peak frequency (ν_m) of a self-absorbed synchrotron source. This assumption means that we are investigating the minimum conditions required to produce the radiation. If the radio source should exhibit a negative slope in the frequency range which we consider, for a given distribution of relativistic particles and fields, the size of the object would have to be increased; if the spectrum has a positive index, then for a given angular size, the characteristic energies of the radiating electrons would have to be greater. Simultaneous radio observations at several frequencies are required to determine whether the present observations actually correspond to the optically thin or the optically thick regimes of the synchrotron spectrum.

Using the spectra shown in Figure 2 for the various values of the parameter N/BA, and the observed flux density of 2×10^{-25} erg $cm^{-2}sec^{-1}Hz^{-1}$

at 5×10^9 Hz, we can compute the values of N, B and A as functions of this parameter. The results are given in Table 1, where R is the radius of the circular area A. As can be seen, as R decreases, B decreases and N increases. From the numerical values in Table 1 we can deduce

$$B \propto R^4 \tag{4}$$

and

$$N \propto R^{-8}. \tag{5}$$

Equations (4) and (5) can also be obtained directly from equations (2) and (3) for $\Gamma = 3$. We should point out, however, that the exponent of R in equation (4) is independent of the spectral index Γ, while in equation (5) it is equal to $-2(\Gamma+1)$.

Using Table 1 and equations (4) and (5) we have computed B and N for a larger range of radii R. We have also computed the number density, n_{rel}, and the energy density, w_{rel}, of the relativistic electrons, as well as the energy density of the magnetic field, w_{mag}. These are shown in Table 2 for various values of R. From this table, and from equations (4) and (5), we see that

$$w_{rel} \propto R^{-11} \tag{6}$$

and

$$w_{mag} \propto R^8. \tag{7}$$

For the stability of the radio-emitting region we require $w_{rel} \lesssim w_{mag}$, which implies that $R \gtrsim 1.6 \times 10^{12}$ cm. This minimum value of R also corresponds to minimum total energy in the relativistic particles and the magnetic field in the radio-emitting region. Much larger values of R

cannot be directly ruled out. They would require, however, that large magnetic fields be spread out over large volumes, which, from energy arguments alone, seems quite unlikely.

The spectra shown in Figure 2 correspond to negligible Razin suppression. From the condition $\nu_R \lesssim \nu_m = 5 \times 10^9$ Hz we can find an upper limit for the ambient electron density which is more stringent than that obtained from the plasma-frequency argument used above. The resultant densities, n_{max}, are also given in Table 2. As can be seen, even for the smallest permissible R (1.6×10^{12} cm), the relativistic electrons constitute only a small fraction of the ambient matter in the radio-emitting region. On the other hand, this ambient density and radius lead to an emission measure of $n_e^2 V = 3 \times 10^{55}$ cm^{-3}, which is more than four orders of magnitude smaller than that required for the low-energy X-rays, but only two orders of magnitude below the emission measure necessary to produce the H_β line (Tucker 1967). This result, therefore, tends to support a model in which the thermal continuum at infrared, visual and X-ray frequencies would be produced in a small, dense core (with a radius perhaps as low as 10^9 cm, as suggested by Neugebauer et al. 1969), whereas the radio emission is generated in a larger volume with radius of the order of 10^{12} cm. The matter in this region could be much cooler than in the dense core and could therefore account for some of the observed line emission from Sco X-1.

The mean energy of the electrons responsible for synchrotron emission at $\nu_m = 5 \times 10^9$ Hz, in a magnetic field of $B \approx 5$ gauss corresponding to

$R \approx 1.6 \times 10^{12}$ cm, is approximately 15 MeV. The characteristic times for synchrotron losses in such a field and collision losses in an ambient plasma of density $n \approx 10^{9}$ cm^{-3} are both of the order of 10^{5} to 10^{8} sec. These times are long compared with the observed time scale for variations in the radio emission of a few hours (Ables 1969). We conclude, therefore, that these variations are probably due to causes other than energy losses of the relativistic electrons. Simultaneous observations of time variations in the radio, optical and X-ray bands could provide important information on the source of these variations. Since the radio-emitting region appears to be different from that responsible for the thermal continuum, the radio variations are probably not strongly correlated with the optical and X-ray fluctuations. They may, however, be more closely related to variations in the line emission as well as in the high-energy non-thermal X-radiation.

REFERENCES

Ables, J. G. 1969, Ap. J. (Letters), 155, L27.

Andrew, B. H., and Purton, C. R. 1968, Nature, 218, 855.

Buselli, G., Clancy, M. C., Davison, P. J. N., Edwards, P. J., McCracken, K. G., and Thomas, R. M. 1968, Nature, 219, 1124.

Chodil, G., Mark, H., Rodrigues, R., Seward, F. D., Swift, C. D., Turiel, I., Hiltner, W. A., Wallerstein, G., and Mannery, E. J. 1968, Ap. J. 154, 645.

Ginzburg, V. L., and Syrovatskii, S. I. 1965, Ann. Rev. Astron. Astrophys., 3, 297.

Ginzburg, V. L., and Syrovatskii, S. I. 1969, Ann. Rev. Astron. Astrophys., to be published.

Gorenstein, P., Gursky, H., and Garmire, G. 1968, Ap. J., 153, 885

Hayakawa, S., Matsuoka, M., and Sugimoto, D. 1966, Space Sci. Rev., 5, 109.

Johnson, H. M. 1966, Ap. J., 144, 635.

Lewin, W. H. G., Clark, G. W., and Smith, W. B. 1968, Can. J. Phys., 46, S409.

Manley, O. P. 1966, Ap. J., 144, 1253.

Neugebauer, G., Oke, J. B., Becklin, E., and Garmire, G. 1969, Ap. J., 155, 1.

Peterson, L. E., and Jacobson, A. S. 1966, Ap. J., 145, 962.

Ramaty, R. 1969, Ap. J., to be published.

Riegler, G. R., Boldt, E. A., and Serlemitsos, P. 1968, Bull. Am. Phys. Soc., 13, 1434.

Riegler, G. R. 1969, Ph. D. thesis, Univ. of Maryland, published as NASA/Goddard Space Flight Center Report X-611-69-1.

Sandage, A. R., Osmer, P., Giacconi, R., Gorenstein, P., Gursky, H., Waters, J., Bradt, H., Garmire, G., Sreekantan, B. V., Oda, M., Osawa, K., and Jugaku, J. 1966, Ap. J., 146, 316.

Tucker, W. H. 1967, Ap. J. (Letters), 149, L105.

Westphal, J. A., Sandage, A., and Kristian, J. 1968, Ap. J., 154, 139.

FIGURE CAPTIONS

Figure 1. The spectrum of Sco X-1. Positive radio measurements were reported by Andrew and Purton (1968) (cross) and by Ables (1969) (circle; the bar indicates the range of observed fluxes). The curves in the optical and X-ray bands are representative of a number of reported measurements. The solid line in the infrared and visual bands represents the data of Neugebauer et al. (1969), the dotted lines correspond to two low-energy X-ray observations of Gorenstein et al. (1968), and the dash-dotted line fits the high-energy X-ray observations of Buselli et al. (1968). The broken line represents the bremsstrahlung spectrum from an isothermal gas at $T = 5 \times 10^7$ ^{o}K, normalized to typical X-ray spectra.

Figure 2. Gyro-synchrotron and synchrotron radiation spectra in vacuum for a radio source with self absorption for given values of the parameter N/BA and the product BN/A. (N - total number of electrons above 100 kev, B - magnetic field, A - effective radiating area of the source). These spectra correspond to radiation from an isotropic electron distribution in a homogeneous and uniform magnetic field, into unit solid angle, 45^{o} to the direction of the field.

TABLE 1

N/BA ($gauss^{-1}\,cm^{-2}$)	BN (gauss)	B (gauss)	N(>100kev)	R (cm)
10^{9}	1.8×10^{41}	7.2×10^{2}	2.5×10^{38}	1.1×10^{13}
10^{11}	1.0×10^{42}	2.8×10^{2}	3.6×10^{39}	6.4×10^{12}
10^{13}	5.6×10^{42}	1.1×10^{2}	5.0×10^{40}	3.8×10^{12}
10^{15}	3.0×10^{43}	3.7×10^{1}	8.1×10^{41}	2.6×10^{12}
10^{17}	1.2×10^{44}	1.1×10^{1}	1.2×10^{43}	1.9×10^{12}
10^{19}	5.3×10^{44}	3.0×10^{0}	1.8×10^{44}	1.4×10^{12}

TABLE 2

R (cm)	B (gauss)	N(>100kev)	n_{rel} (cm^{-3})	w_{rel} ($erg.cm^{-3}$)	w_{mag} ($erg.cm^{-3}$)	n_{max} (cm^{-3})
1.0×10^{13}	6.6×10^{2}	3.5×10^{38}	8.4×10^{-2}	2.7×10^{-6}	1.7×10^{4}	1.6×10^{11}
3.2×10^{12}	6.0×10^{1}	2.5×10^{41}	1.9×10^{3}	6.0×10^{-4}	1.4×10^{2}	1.5×10^{10}
1.6×10^{12}	5.2×10^{0}	5.7×10^{43}	3.5×10^{8}	1.1×10^{0}	1.1×10^{0}	1.3×10^{9}
1.0×10^{12}	8.5×10^{-1}	2.2×10^{45}	5.3×10^{8}	1.7×10^{2}	2.9×10^{-2}	2.1×10^{8}
3.2×10^{11}	8.5×10^{-3}	2.2×10^{49}	1.7×10^{14}	5.3×10^{7}	2.9×10^{-6}	2.1×10^{6}
1.0×10^{11}	8.5×10^{-5}	2.2×10^{53}	5.3×10^{19}	1.7×10^{13}	2.9×10^{-10}	2.1×10^{4}

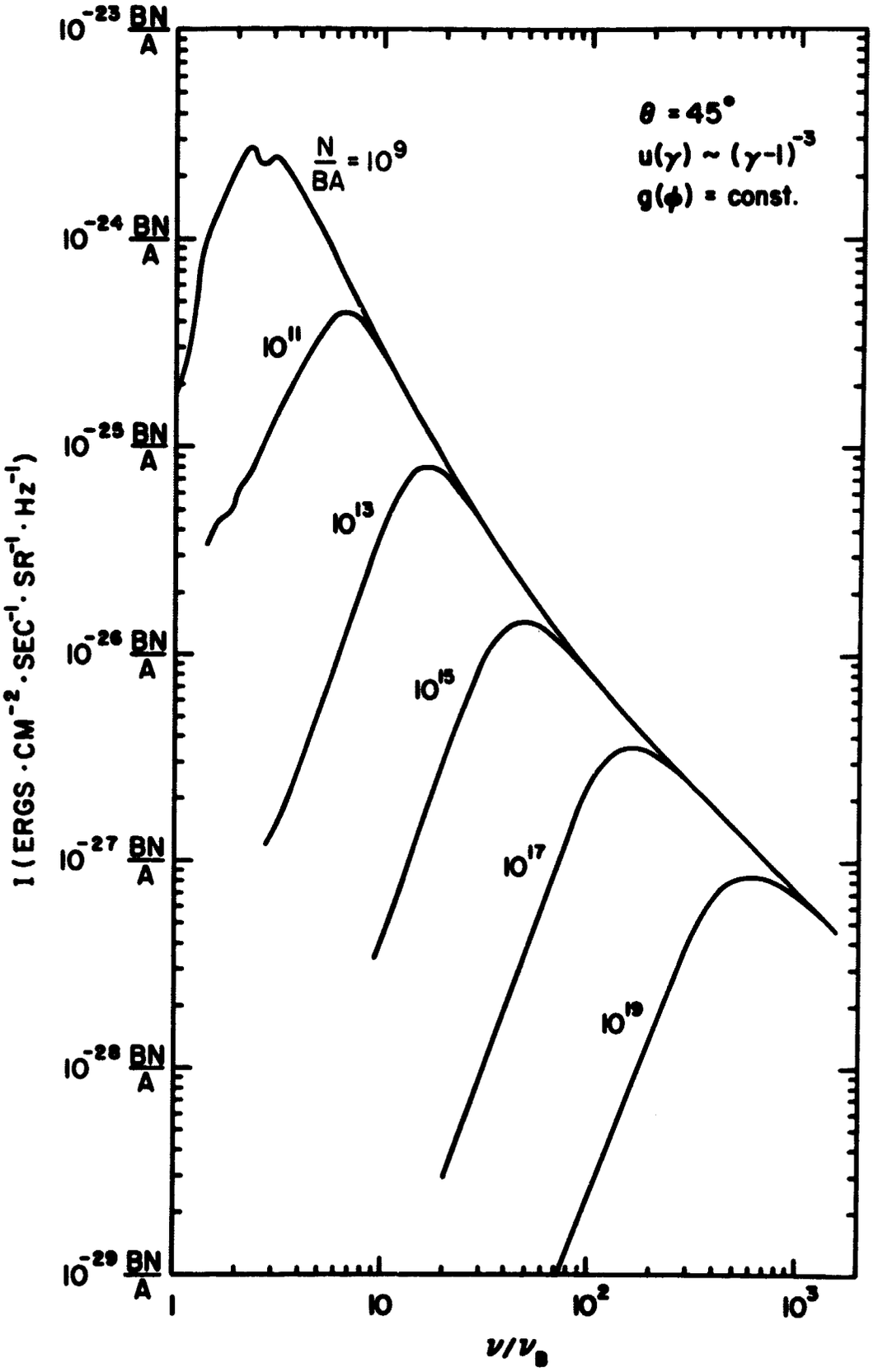
$10^{-23}\frac{BN}{A}$
$10^{-24}\frac{BN}{A}$
$10^{-25}\frac{BN}{A}$
$10^{-26}\frac{BN}{A}$
$10^{-27}\frac{BN}{A}$
$10^{-28}\frac{BN}{A}$
$10^{-29}\frac{BN}{A}$
$I\,(ERGS\cdot CM^{-2}\cdot SEC^{-1}\cdot SR^{-1}\cdot Hz^{-1})$
$\theta = 45°$
$u(\gamma) \sim (\gamma-1)^{-3}$
$g(\phi) = \text{const.}$
$\frac{N}{BA} = 10^{9}$
10^{11}
10^{13}
10^{15}
10^{17}
10^{19}
1
10
10^{2}
10^{3}
ν/ν_B

Figure 1

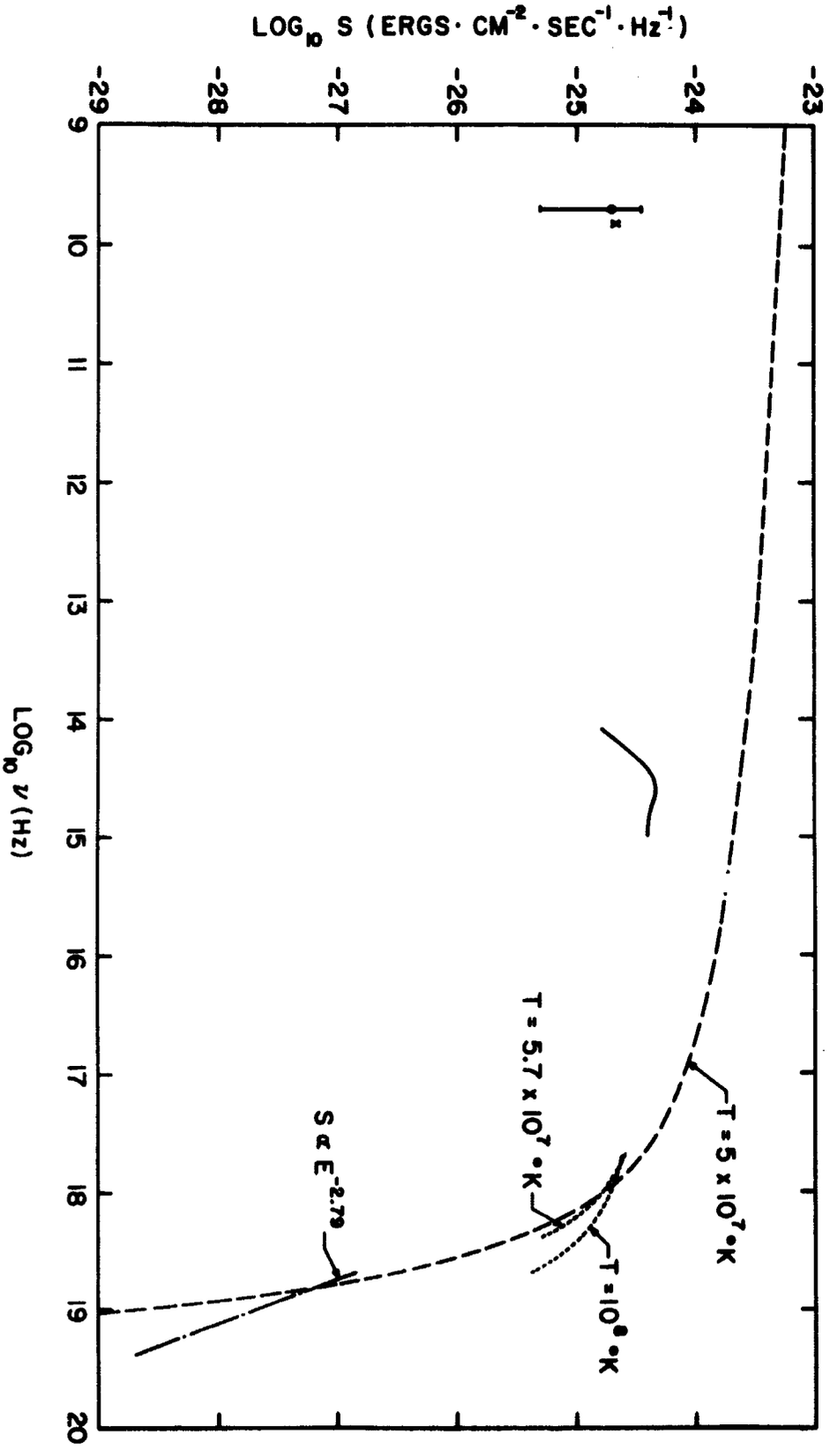
LOG₁₀ S (ERGS · CM⁻² · SEC⁻¹ · Hz⁻¹)
-29
-28
-27
-26
-25
-24
-23
9
10
11
12
13
14
15
16
17
18
19
20
LOG₁₀ ν (Hz)
S ∝ E^-2.79
T = 5.7 x 10⁷ °K
T = 10⁸ °K
T = 5 x 10⁷ °K

Figure 2